





Article

Study on Water and Salt Transport under Different Subsurface Pipe Arrangement Conditions in Severe Saline–Alkali Land in Hetao Irrigation District with DRAINMOD Model

Feng Tian ^{1,2,†}, Qingfeng Miao ^{1,2,†} , Haibin Shi ^{1,2,*}, Ruiping Li ^{1,2}, Xu Dou ^{1,2} , Jie Duan ^{1,2}, Jing Liu ³  and Weiyang Feng ^{4,*} 

¹ College of Water Conservancy and Civil Engineering, Inner Mongolia Agricultural University, Hohhot 010010, China; tianfeng@emails.imau.edu.cn (F.T.); 15049121836@126.com (Q.M.); nmglrp@163.com (R.L.); nmgdouxu@163.com (X.D.); nmgyuanjie@163.com (J.D.)

² High Efficiency Water-Saving Technology and Equipment and Soil and Water Environment Effect in Engineering Research Center of Inner Mongolia Autonomous Region, Hohhot 010011, China

³ Environment Research Institute, Shandong University, Qingdao 266237, China; liu_jing@email.sdu.edu.cn

⁴ School of Materials Science and Engineering, Beihang University, Beijing 100191, China

* Correspondence: shb@imau.edu.cn (H.S.); fengweiyang@buaa.edu.cn (W.F.)

† These authors contributed equally to this work.

Abstract: As an effective method to improve saline–alkali land, the drainage from subsurface pipes has been extensively studied in typical arid and semi-arid agricultural areas (Hetao Irrigation District). However, there are few studies on the improvement of subsurface pipe layout and the long-term soil salinization control in the process of leaching and soil amendment with subsurface pipes in this area. This study investigated the water and salt migration in the process of amending the heavy saline soil. Field experiments growing sunflowers and numerical model calculation were combined in this research. It was found in the field experiment that the salt concentration in the surface pipe drainage was positively correlated with the salt content in the soil and the depth of the pipe, while it was negatively correlated with the amount of irrigation water and the spacing of crops. Thus, the soil desalting rate (N) and salt control rate (SCR) were positively correlated with the depth of the pipe, and they were negatively correlated with the spacing. The leaching effect of irrigation would decrease when the soil salt content decreased. On the basis of field experiments, the DRAINMOD model and drainmod equation were used to calculate the water and salt migration in 38 different field plots during 2019 and 2020. When N was the same, the soil salinity in several plots with large burial depth could be controlled below the salt tolerance threshold of sunflowers during the growth period in the second year. The quantitative relationship between N and SCR , soil salt content before leaching, water amount of leaching, pipe spacing and buried depth was already established. These results can help develop strategies for desalination and salt control in the soil in the arid and semi-arid areas with the optimal layout of subsurface pipes.

Keywords: Hetao Irrigation District; saline–alkali soil; subsurface drainage system; DRAINMOD; water and salt transport



Citation: Tian, F.; Miao, Q.; Shi, H.; Li, R.; Dou, X.; Duan, J.; Liu, J.; Feng, W. Study on Water and Salt Transport under Different Subsurface Pipe Arrangement Conditions in Severe Saline–Alkali Land in Hetao Irrigation District with DRAINMOD Model. *Water* **2023**, *15*, 3001. <https://doi.org/10.3390/w15163001>

Academic Editor: William Frederick Ritter

Received: 14 July 2023

Revised: 13 August 2023

Accepted: 18 August 2023

Published: 20 August 2023



Copyright: © 2023 by the authors. Licensee MDPI, Basel, Switzerland. This article is an open access article distributed under the terms and conditions of the Creative Commons Attribution (CC BY) license (<https://creativecommons.org/licenses/by/4.0/>).

1. Introduction

As a global agricultural issue, soil salinization has been widely concerned because it reduces the utilization efficiency of fertilizers, increases the loss of nutrients in the soil, and affects the growth, yield and quality of crops [1–5]. Soil salinization has affected more than 30% of arid and semi-arid areas worldwide [6,7]. As a typical arid and semi-arid irrigated area, 63.8% of the soil in the Hetao Irrigated District of Inner Mongolia has been affected by salinization [8]. Subsurface pipe drainage has been widely recognized as an effective measure for amending saline farmland [9], due to its advantages of small land

occupancy and high land use efficiency for improving soil conditions, reducing soil salinity and increasing crop yield [10–12]. There have been many studies on the displacement, drainage quality and the influence on groundwater level of the subsurface pipe with different layout parameters [13,14]. However, the proposed layout parameters in those studies may not be applicable to the area for desalting and long-term salt control in the arid and semi-arid areas.

The key points of the research on the subsurface pipe mainly include the drainage, salt and nutrient transport, the response of crop yield, and the optimal layout parameters of subsurface pipes under different soil conditions [15–17]. Many studies have carried out quantitative analysis of various farmland indicators with different layout parameters of subsurface pipes. Laboratory and field experiments showed that the depth of subsurface pipe positively affected the quantity and quality of discharged water, while the spacing of subsurface pipe presented negative influence on these parameters [18,19].

The migration of water and salt under different pipe layout conditions cannot be fully investigated due to the limitations of laboratory and field tests. The numerical model is an effective and complementary method to solve this issue. Some of the effective and widely accepted models include but are not limited to the HYDRUS [20], SWAT [21] and DRAINMOD [22]. Dou et al. used HYDRUS-2D to simulate the subsurface pipe drainage in the farmland compared the drainage depth of the subsurface pipe at different growth stages of sunflowers, and they determined that the optimal drainage depth in medium salinized soil was 50 cm [23]. Addab and Bailey simulated the migration of eight major salt ions in the soil with subsurface pipe drainage in the salinized area, and they developed effective land and water management strategies with the SWAT model [24,25]. DRAINMOD, based on water balance, is widely used to simulate farmland drainage and crop yield because of its simplicity, accuracy and practicability [26,27]. The model was extended to simulate the macropore seepage [28]. Meanwhile, this model well simulated the recycling of subsurface pipe drainage water and the related economic benefits [29].

Hetao Irrigation District is a typical salinization area, and many studies have been conducted on the improvement of soil quality in this region [30,31]. However, few studies focused on the subsurface pipe drainage and the water and salt migration in the soil with subsurface pipes in long time series. The groundwater level is high, and soil permeability is poor in the heavily salinized area. As a result, the salinity of the soil can only be reduced in a short period of time even if subsurface drainage is used. This study mainly investigated the water and salt migration in the salinized farmland growing sunflowers with buried drainage pipes in Hetao Irrigation District. Based on this field experiment, simulation was conducted with DRAINMOD model for water migration and calculate the soil salt migration. The index of salt control rate (SCR) was proposed to describe the effect of subsurface pipe on the salinity of main root layer soil of sunflowers, and the best arrangement of the subsurface pipe under different desalting and salt control requirements with planting sunflower was determined to provide technical support for the improvement of subsurface pipe drainage in the arid and semi-arid areas.

2. Materials and Methods

2.1. Study Site

From May 2019 to November 2020, a trial of leaching was conducted in a field with an area of approximately 5.4 ha. The field is located in the Comprehensive Improvement Test Base of Saline–alkali Land with Subsurface Pipe Drainage in the Wulat irrigation area, Hetao Irrigation District, Inner Mongolia, northwest China, with an altitude of 1018.88 m at 40°45′28″ N and 108°38′16″ E [32]. The region has a typical temperate continental climate, dry and windy, with an annual evaporation of 2173 mm [33]. The groundwater is relatively shallow with a depth of 1.6 m, and the salinity of groundwater is 29.66 dS/m. Flood irrigation is mainly used for irrigation with water from the Yellow River with a total dissolved solids content of 0.67 g/L. The drainage method is mostly open ditch, which is mostly used for drainage in this area. The large amount of irrigation water use, untimely

drainage, high groundwater level and intense surface evaporation lead to prominent soil salinization and seriously restrict the development of local agriculture.

2.2. Field Test Design

Seven test fields were constructed. The Dutch INTERDRAIN all-in-one pipe laying machine was used to complete the ditching and laying of the subsurface pipes, which were single-wall bellows pipes with a diameter of 8 cm, a length of 200 m and a buried slope of 1‰. The pipes were arranged in the short direction of the field, and then they were wrapped with geotextiles, covered with sand of 10 cm, backfilled with original soil to the initial elevation, and finally processed via laser leveling.

The leaching water was discharged from the subsurface pipe to the drainage ditch excavated along one side of the field. Referring to previous studies [34], the drainage depth of the pipes was set at 1.1 m, 1.2 m and 1.3 m, and the drainage spacing was set at 10 m, 20 m and 30 m. Seven field experiments were arranged, as shown in Figure 1a. Due to the limitation of field tests, the drain depth ranged from 1.1 m to 1.3 m, and the drain spacing ranged from 10 m to 30 m. DRAINMOD model was used to simulate the desalination and salt control effects of different layout parameters of the pipes under the same initial soil conditions. There were a total of 38 prediction scenarios, denoted as F_1 – F_{38} , with 9 drain depths (1 m, 1.1 m, 1.2 m, 1.3 m, 1.4 m, 1.5 m, 1.6 m, 1.8 m and 2 m) and 5 drain spacings (10 m, 15 m, 20 m, 25 m and 30 m). Field and prediction layout of subsurface pipes are shown in Table 1.

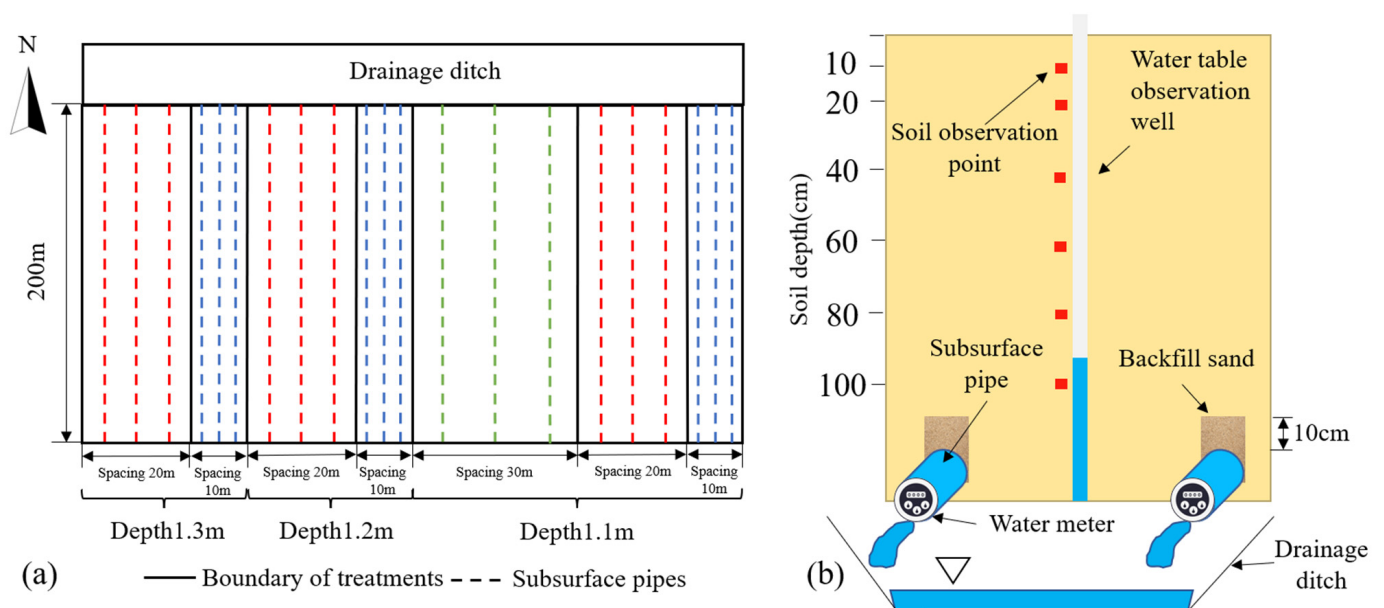


Figure 1. Schematic diagram of (a) subsurface drainage pipe layout of each treatment and (b) drainage structure of subsurface pipe and observation point of water and soil samples (The green line is a subsurface pipe with a spacing of 30 m. The red line is a subsurface pipe with a spacing of 20 m. The blue line is a subsurface pipe with a spacing of 10 m).

2.3. Sampling, Measurement and Calculation

2.3.1. Meteorological Data

The weather input files required by the model included precipitation, solar radiation, maximum and minimum temperatures, wind speed, etc. The hourly data were obtained from field weather stations (HOBO-U30) used at the test field.

Table 1. Layout parameters of the 7 experiment (T) and 38 prediction (F) scenarios.

Depth (cm)	Spacing (cm)				
	1000	1500	2000	2500	3000
100	F ₁	F ₂	F ₃	F ₄	F ₅
110	T ₁	F ₆	T ₄	F ₇	T ₇
120	T ₂	F ₈	T ₅	F ₉	F ₁₀
130	T ₃	F ₁₁	T ₆	F ₁₂	F ₁₃
140	F ₁₄	F ₁₅	F ₁₆	F ₁₇	F ₁₈
150	F ₁₉	F ₂₀	F ₂₁	F ₂₂	F ₂₃
160	F ₂₄	F ₂₅	F ₂₆	F ₂₇	F ₂₈
180	F ₂₉	F ₃₀	F ₃₁	F ₃₂	F ₃₃
200	F ₃₄	F ₃₅	F ₃₆	F ₃₇	F ₃₈

2.3.2. Irrigation Time and Water Volume

Flood irrigation was used in the study. The quantity of irrigation water was controlled by installing a circular inlet gate of each plot for measuring the inlet water quantity. The time and frequency of irrigation mainly depend on the local Yellow River inflow time and irrigation management system. During the experiment, seven times of irrigation with different water amounts were carried out, respectively, on 15 May 2019 (300 mm), 26 June 2019 (150 mm), 17 July 2019 (150 mm), 25 October 2019 (300 mm), 3 May 2020 (350 mm), 28 June 2020 (250 mm) and 19 October 2020 (350 mm).

2.3.3. Soil Sampling

In order to monitor the desalination effect of subsurface pipes, soil sampling was conducted one day before each drainage test and after the end of drainage. The soil sampling points were arranged at the intermediate points between the middle subsurface pipe and the adjacent subsurface pipe in each test area. The surface soil was sampled from 0–10 cm and 10–20 cm, and then the soil was sampled every 20 cm below the surface to a depth of 100 cm (Figure 1b).

2.3.4. Water Sampling

A water meter was connected to the subsurface pipe near the drain. In order to facilitate water meter disassembly and data collection, A manhole was built above water meter. The daily subsurface pipe displacement and drainage quality were monitored during the irrigation and drainage stage.

2.3.5. Water Table

Groundwater level observation wells were arranged near the soil sampling points in each test plot. Meter ruler and plumb hammer were used to measure the groundwater level in the initial stage of the test, and a groundwater level monitor DATA-6216 was placed in the observation wells to monitor the real-time groundwater level during the test.

2.3.6. Soil Moisture Content, Salt Content, Desalting Rate and Salt Control Rate

Some soil samples were weighed to determine the wet weight and then dried in a hot blast oven at 105 °C for 24 h to measure the dry weight and calculate the moisture content. Next, 10 g of some soil sample was well mixed in 50 mL distilled water. After standing for 15 min, the conductivity of the solution (*EC*) was measured using a lightning magnetic DDS-307A conductivity meter. The soil salt content was obtained using Equation (1) [35]. The soil desalting rate was calculated using Equation (2) [23].

$$S = 3.7657EC_{(1:5)} - 0.2405 \quad (1)$$

where S is soil salt content (g/kg), and $EC_{1.5}$ is the EC of the soil extract solution made by mixing the soil with water at a soil:water ratio of 1:5, (mS/cm).

$$N = \frac{S_1 - S_2}{S_1} \times 100\% \quad (2)$$

In the equation, N is the soil desalting rate (%), S_1 is the initial value of soil salinity before irrigation (g/kg), and S_2 is the soil salinity after irrigation (g/kg).

The index of salt control rate (denoted as SCR), proposed in this study, represents the percentage of days when the salinity in the soil was lower than the threshold of crop salinity in the total growth period, which was used to reflect the control ability of subsurface pipe drainage on soil salinity, so as to select the suitable subsurface pipe layout.

2.4. DRAINMOD Model

2.4.1. Model Description

DRAINMOD is a two-dimensional model to obtain information of soil hydrological processes using a water balance method and empirical relationships with data about meteorology, soil properties, crop growth and field irrigation/drainage [22]. An hourly or daily simulation of the water balance at the midpoint of two parallel drainage pipes, including evapotranspiration, surface runoff, subsurface drainage, infiltration and groundwater level. The salt module of the model is rarely used because the calculation process is not rigorous, resulting in a large difference between the simulation results and the actual situation. This paper only uses it for hydrological simulation.

Water balance in this model is classified as two compartments: In the surface balance, the model can be applied to compute the permeability, irrigation and runoff using the following Equation (3). In the subsurface balance, DRAINMOD calculates the water balance for a section of the soil in the middle of two drains according to the following Equation (4) [22].

$$\Delta W = P + I - F - RO \quad (3)$$

$$\Delta V_a = D + ET + VLS - F \quad (4)$$

In the equation, ΔW is the change in surface water storage (mm); P is the precipitation (mm); I is the irrigation amount (mm); F is the infiltration amount (mm); RO is the surface runoff (mm); ΔV_a is the change in water content of anhydrous pore space in soil profile (mm); D is the drainage depth (mm); ET is the evapotranspiration (mm); and VLS is the vertical and lateral flow (mm).

The flow from spawn to sink to drain was assumed instantaneous in the DRAINMOD model. The amount of irrigation water was measured in the field. The amount of infiltration was estimated with Green–Ampt equation with the input of soil physical properties. In the equation, surface runoff was not included since all the irrigation water was discharged from the field through subsurface drainage due to the 1 m high ridge surrounding the field. The efficiency of subsurface drainage depends on the depth of groundwater, soil hydraulic conductivity and the layout of buried pipes. When the underground water level is below the surface, Hooghoudt steady flow equation is used to calculate the underground pipe displacement; when the underground water level rises to completely submerge the ground, the Kirkham equation is used to estimate the underground drainage flow [36]. Vertical and lateral seepage were estimated using a simple method based on the Darcy equation and Dupuit-Forchheimer hypothesis [22,37].

2.4.2. Model Input

The selected field was an abandoned farmland. A comprehensive soil survey was carried out before burying the pipes (Table 2). The drainage depth and spacing of the field drainage system depended on the buried subsurface pipe parameters in each test area. The depth from the surface to the impermeable layer was set to 2 m, the initial depth of the groundwater was set to the actual measured value (160 cm), and the depth at which

water flows to the subsurface pipe (Kirkham depth) was set to 0.3 cm. The actual irrigation time and irrigation amount are integrated into the meteorological data and then input into the model. The model calculates the potential evapotranspiration (PET) based on the input meteorological data and the Penman–Monteith formula, and then it distributes the calculated PET to each hour of the simulation period. In the calculation process, the model will self-check whether evapotranspiration is limited by soil moisture conditions. If it is not affected by soil water supply capacity, the actual evapotranspiration (ET) is equal to PET . Otherwise ET is equal to soil water supply capacity (upward flux of diving).

Table 2. Soil physical and chemical characteristics of experimental site.

Soil Layer (cm)	Particle Composition/%			Bulk Density ($\text{g}\cdot\text{cm}^{-3}$)	Soil Salt Content ($\text{g}\cdot\text{kg}^{-1}$)	pH	Field Capacity ($\text{cm}^3\text{ cm}^{-3}$)
	Sand	Clay	Silt				
0–10	36.6	4.22	59.18	1.44	25.23	7.45	32.35
10–20	32.32	3.86	63.82	1.45	21.79	7.60	33.29
20–40	23.98	2.20	73.82	1.47	18.22	7.64	36.61
40–60	8.27	2.47	89.26	1.48	15.53	7.72	35.08
60–80	3.36	5.70	90.94	1.49	11.79	7.51	36.33
80–100	12.91	5.02	82.07	1.49	10.60	7.62	36.52

As one of the main planting cash crops in Hetao Irrigation District, sunflowers have high salt tolerance (18.28 g/kg) and are generally sown in early June and harvested in early or middle September, with a growth period of about 105 d. The irrigation water in this study was from the Yellow River, and the time of each irrigation test was consistent with the local irrigation schedule. The potential evapotranspiration of bare land is PET_1 . In order to simulate the soil water balance when sunflowers were planted, the dual crop coefficient [38,39] method was used to calculate crop transpiration (T_c) and soil evaporation (E_s), respectively, to estimate potential evapotranspiration (PET_2) during sunflower planting.

$$T_c = K_{cb}ET_o \quad (5)$$

$$E_s = ET_o \quad (6)$$

Here, K_{cb} is the basal crop coefficient; K_e is soil evaporation coefficient; and ET_o is the reference crop evapotranspiration.

Basal crop coefficient refers to the ratio of crop evapotranspiration to reference evapotranspiration at a given potential rate without soil evaporation. Miao et al. provided the K_{cb} reference values in the early (0.10), middle (1.15) and late (0.25) growth periods of sunflower after calibration [40]. The evaporation coefficient K_e is used to describe the portion of soil evaporation in the actual evapotranspiration, which depends on the amount of water available for evaporation in the upper soil and on the amount of energy available at the soil surface in conjunction with the energy consumed by transpiration [41].

$$K_e = K_r (K_{c\max} - K_{cb}) \leq f_{ew} K_{c\max} \quad (7)$$

In the equation, K_r is the evaporation reduction coefficient, depending on the cumulative depth of surface soil water loss, and $K_{c\max}$ is the maximum value of K_c after rainfall or irrigation. The calculation of K_r is divided into two stages. When the accumulated evaporation loss from soil surface (D_e , mm) does not exceed the amount of evaporable water (REW , mm), K_r is equal to 1. When D_e exceeds REW , K_r decreases, and when the evaporation from surface soil is 0, $K_r = 0$. Equation (8) was used to calculate the K_r of the second stage.

$$K_r = \frac{TEW - D_{e,i-1}}{TEW - REW} \quad (8)$$

In the equation, TEW is the maximum depth of evaporation of surface soil after wetting (mm); REW is the amount of water easily evaporated without water limitation (the

cumulative evaporation depth at the end of the first stage); $D_{e,i-1}$ is the cumulative depth of soil surface evaporation water at the end of day $i-1$ (mm).

f_{ew} is the fraction of soil that is exposed to radiation and moistened by water, and it is related to the percentage of the ground covered by crops.

$$f_{ew} = \min(1 - f_c, f_w) \quad (9)$$

In the equation, f_c is the fraction of the surface soil area covered by plants. f_w is the fraction of soil surface wetting by rainfall or irrigation.

2.5. Water and Salt Balance in Soil Profile

In the calculation of water balance in the soil profile of the test site including shallow groundwater utilization, the influence of soil pore distribution difference on water migration is ignored for the convenience of the study, and the piston flow is considered. When calculating the water amount of precipitation, irrigation, underground drainage, shallow groundwater utilization, evapotranspiration and infiltration, the salt carried in each part of water is defined to clarify the water-salt balance of the profile. The calculation formula is as follows:

Moisture:

$$\Delta V_a = P + I + G - D - ET - L \quad (10)$$

Salt:

$$S = S_O + S_I + S_G - S_D - S_L \quad (11)$$

In the equation, G is the utilization of shallow groundwater (cm); L is the deep percolation (cm); S_O is the initial salt content of soil profile (g); S_I is the salt brought by irrigation water (g); S_G is the rising salinity by groundwater (g); S_D is the salt discharged by underground drainage (g); S_L is the salt introduced into groundwater (g).

When the water table rises after rain or irrigation, the water quantity L of deep seepage can be calculated using the following equation.

$$L = \mu \Delta H \quad (12)$$

Here, μ is the water supply degree. According to experience, the value of μ in the test site ranges from 0.04 to 0.06 [42], calibrated via moisture calculation, and the value in this paper is 0.05. ΔH is the change in depth of groundwater after rainfall or irrigation (cm).

The salt brought into groundwater can be calculated using Equation (13):

$$S_L = \frac{S_O + S_I}{V_a + L} \quad (13)$$

where V_a is the moisture content of soil before rainfall or irrigation.

2.6. Shallow Groundwater Utilization and Salt Accumulation Rate

The simulation was carried out under the two conditions, i.e., the bare land and land with crops. Under the two conditions, the corresponding underground displacements were D_1 and D_2 , evapotranspirations were ET_1 and ET_2 , infiltrations were F_1 and F_2 , deep percolation were L_1 and L_2 , and groundwater levels were h_1 and h_2 (usually $h_1 < h_2$). The difference in the profile water quantity between bare land and land with planted crops was mainly caused by the utilization of groundwater by crops. Therefore, by calculating the difference in water balance between the two conditions, the amount of shallow groundwater used by crops can be obtained using Equation (14).

$$G = (D_1 - D_2) + (ET_1 - ET_2) + (F_2 - F_1) + (L_2 - L_1) + (h_2 - h_1)\theta_s \quad (14)$$

In the equation, θ_s is the saturated water content ($\text{cm}^3 \text{cm}^{-3}$). Equation (15) can be used to obtain the total amount of salt carried by crops using groundwater, and Equation

(16) can be used to calculate the salt accumulation rate of soil, and the salt accumulation degree (soil profile at a certain time and the rate of increase in soil salt content compared to the previous period) of 0–100 cm soil layer in each test plot is analyzed without being affected by the initial salt content.

$$S_G = GC_G \quad (15)$$

Here, C_G is the average salt concentration of groundwater.

$$t = \frac{S_i - S_{i-1}}{S_i} \times 100\% \quad (16)$$

In the equation, t is soil salt accumulation rate (%); S_i is the soil salt content in period i (g/kg); and S_{i-1} is the soil salt content in period $i-1$ (g/kg).

2.7. Calibration and Verification of the Models and Fitting Equations

The model was evaluated using graphical and statistical methods. The mean absolute error (MAE), root mean square error (RMSE) and Nash–Sutcliffe efficiency coefficient (NSE) were used to evaluate the consistency between the measured and the predicted data. When MAE and RMSE are close to 0, NSE is close to 1, indicating that the simulation is accurate. When daily NSE > 0.4 or monthly NSE > 0.5, the simulation is considered acceptable; when daily NSE > 0.6 or monthly NSE > 0.7, the simulation is considered good; when daily NSE > 0.75 or monthly NSE > 0.8, the simulation is considered excellent [22].

$$MAE = \frac{\sum_{i=1}^n |A_i - O_i|}{n} \quad (17)$$

$$RMSE = \sqrt{\frac{1}{n} \sum_{i=1}^n (A_i - O_i)^2} \quad (18)$$

$$NSE = 1 - \frac{\sum_{i=1}^n (A_i - O_i)^2}{\sum_{i=1}^n (A_i - \bar{O})^2} \quad (19)$$

The coefficient of determination (R^2) was used to evaluate the regression equation.

$$R^2 = \frac{(\sum_{i=1}^n (O_i - \bar{O})(A_i - \bar{A}))^2}{\sum_{i=1}^n (O_i - \bar{O})^2 \sum_{i=1}^n (A_i - \bar{A})^2} \quad (20)$$

where A_i is the simulated value; \bar{A} is the average observed value; O_i is the average simulated value; \bar{O} is the average observed value; and n is the total number of the observations. The R^2 value is between 0 and 1, and it is acceptable when the value is larger than 0.5.

3. Results and Analysis

3.1. Changes in Soil Water Content and Salinity

The measured soil moisture content and soil salt content of the profile before and after each irrigation test of seven field-arranged experimental treatment plots during the period 2019–2020 were, respectively, provided in Figures 2 and 3. At the beginning of the experiment, there was little difference in the initial water content of each soil layer in each plot. The average soil water content of 0–100 cm soil layer was 36.85–37.89 cm³cm⁻³, and the soil water content of the profile gradually increased with the soil depth. After irrigation, the water content of the profile increased, and the water distribution from the top to the bottom tended to be uniform. With the increase in the buried depth or the decrease in

the distance between the buried pipes, the water discharge rate from the soil accelerated gradually. With the same spacing, the average soil moisture content of 0–100 cm soil layer in the test plot after leaching decreased by $0.54 \text{ cm}^3 \text{ cm}^{-3}$ for every 0.1 m increase in the burial depth. The average soil moisture content of 0–100 cm soil in the test plot increased by $0.08 \text{ cm}^3 \text{ cm}^{-3}$ when the burial depth remained unchanged, and the spacing increased by 10 m. Before the irrigation test, the average salt content in 0–100 cm soil layer of each test plot was 16.93–17.56 g/kg, which gradually decreased with the burial depth, and the spatial variability of soil salt content was large in the same profile (Figure 3). After each leaching test, the soil salt content in each plot showed similar decreasing trends, but the spatial variability was still large. During the interval of two leaching tests, the salt content of the profile increased under the joint influence of surface evaporation and soil capillarity, and the most significant increase occurred in the 0–40 cm soil layer. From 4 June to 25 June 2019, the average salt content increased by 0.53–1.01 g/kg in the 0–100 cm soil layer in each plot, and the average salt content increased by 0.81–2.79 g/kg in the 0–40 cm soil layer. No leaching was carried out from November 2019 to May 2020, but the overall salt content of the soil decreased. This was because the water in the soil melted and carried part of the salt out of the soil, and the salt in the 0–40 cm layer of the surface layer significantly decreased. The soil moisture content and salt content in T₃ plot were significantly lower than those in other plots during the experiment, while those in T₇ plot were higher than those in other plots (Figures 2 and 3). Water discharge led to a more obvious reduction in soil salinity with a deeper burial depth and smaller spacing of the subsurface pipes. Moreover, the influence of subsurface pipe on the surface 0–40 cm soil layer was more significant compared to other layers, and the difference between the water content and salt content of deep soil in the subsurface pipe is small among different plots.

3.2. The Salt Content and Soil Desalting Rate under Experimental Conditions and the Influencing Factors

Linear regression was carried out between the salt concentration of the drainage in the subsurface pipe (C_D) and the soil salt content (S_0), irrigation amount (I), spacing (s) and buried depth (d) as shown in Equation (21).

$$C_D = 5.057S_0 - 0.086I - 0.016s + 0.531d - 39.848 \quad (21)$$

The statistical parameters of the regression model are shown in Table 3. The soil salt content before leaching and the buried depth of pipes had a significant positive influence on the salt concentration of drainage, and the irrigation amount and spacing of the pipes had a significant negative influence on the salt concentration of drainage. After each leaching, the soil salt content varied greatly across the test plots. To compare the changes in the soil salt content, Equation (2) was used to calculate and list the N of each plot after each leaching. N was the desalting capacity of subsurface pipes under different layout conditions without considering leaching (Table 4). After the arrangement of the subsurface pipe, the soil was desalted by irrigation in each plot, and the N range was 10.83–37.94%. N decreased with the increase in pipe spacing when the burial depth of pipes was the same. With the same spacing, N increased with the increase in burial depth. However, the change in soil salt content did not show a similar trend with N . After the irrigation test on 3 May 2020, the highest N was 37.94% in T₃ plot, but the change in soil salt content was 2.36 g/kg, which was lower than that in other plots. The maximum change in soil salt content in T₄ plot was 2.65 g/kg, and N was only 23.31%. With the progress of the experiment, the salt content of the soil in the test plot decreased as a whole, it was more difficult to discharge the salt from the soil, and the leaching effect of the subsurface pipe on the soil also decreased.

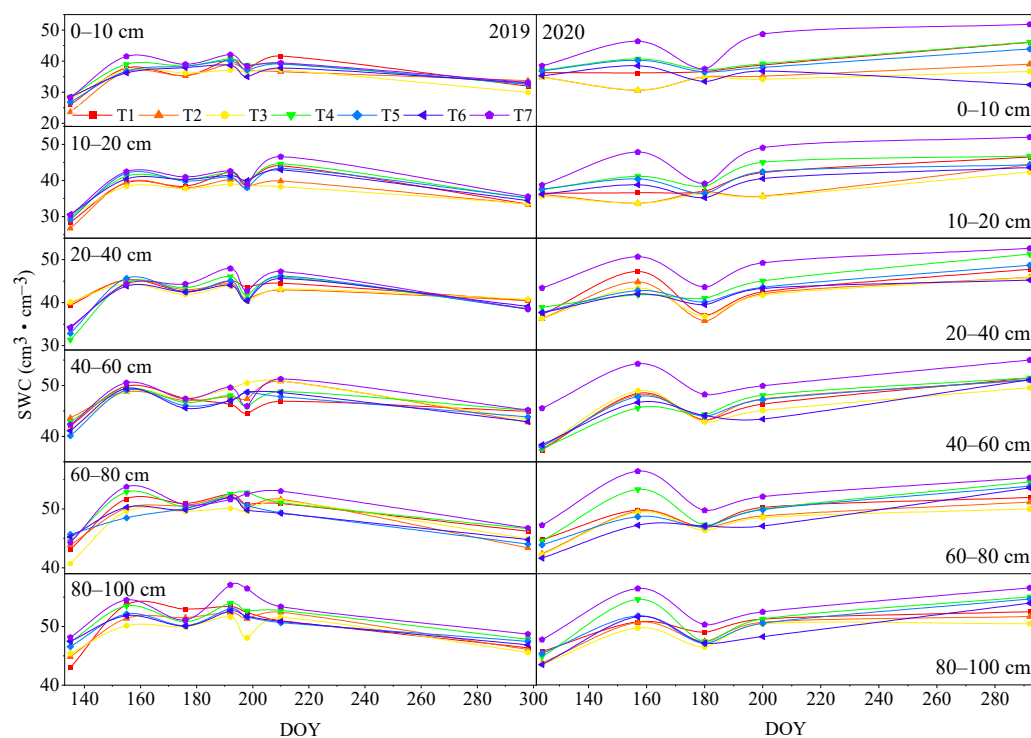


Figure 2. Changes in soil water content (SWCs) of different soil layers in each test plot in 2019 and 2020.

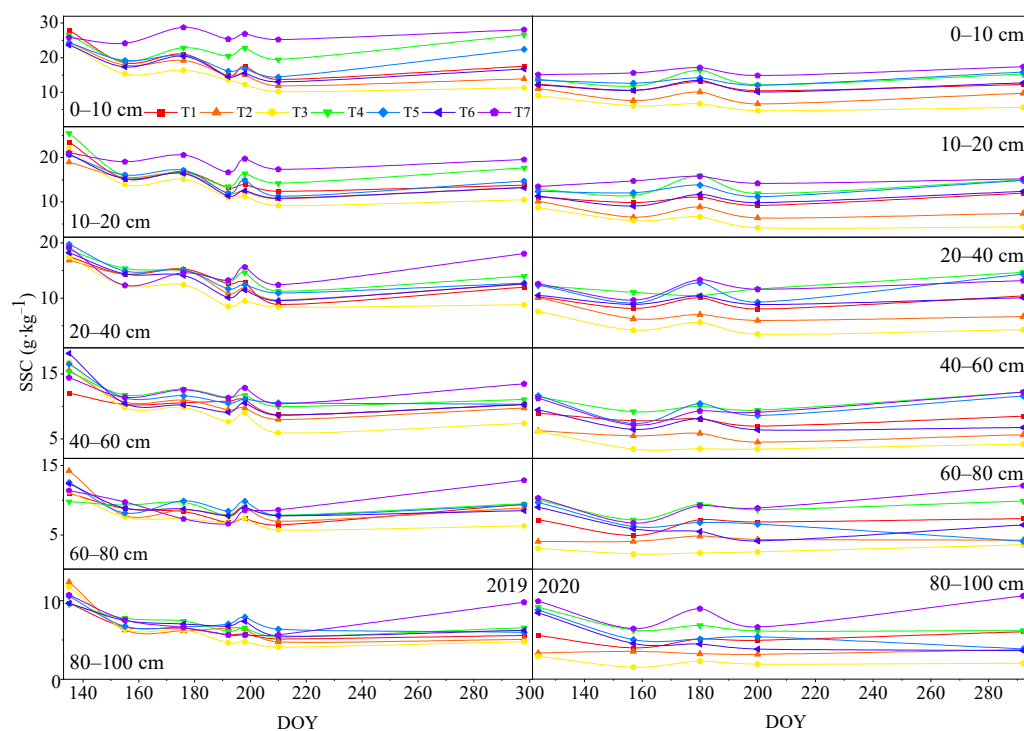


Figure 3. Changes in soil salt content (SSCs) in different soil layers in each test plot in 2019 and 2020.

Table 3. Multiple linear regression model test and parameter statistics for salt concentration in subsurface pipe drainage.

Parameter	Denormalization	Standardization	VIF	<i>p</i>	<i>R</i> ²	<i>F</i>
	Coefficient	Coefficient				
	B	Beta				
Constant	−39.848	-	-	0.018 *		
S _o	5.057	0.811	1.307	0.000 **	0.902	F = 101.123 <i>p</i> = 0.000 **
I	−0.086	−0.344	1.070	0.000 **		
s	−0.016	−0.577	1.298	0.000 **		
d	0.531	0.224	1.125	0.000 **		

Note: *, *p* < 0.05; **, *p* < 0.01.**Table 4.** Change in soil salt content and desalination rate in each test plot after leaching in 2019–2020.

Treatment	Time	Soil Salt Content Change (g·kg ^{−1})	Soil Desalination Rate (%)	Time	Soil Salt Content Change (g·kg ^{−1})	Soil Desalination Rate (%)	Time	Soil Salt Content Change (g·kg ^{−1})	Soil Desalination Rate (%)
T ₁	15 May 2019	4.64	27.38	26 June 2019	2.45	18.75	17 July 2019	2.19	19.25
T ₂		4.98	29.23		2.49	19.51		2.08	19.40
T ₃		6.36	36.93		2.55	22.71		1.78	19.77
T ₄		4.42	25.19		2.02	14.39		2.14	15.86
T ₅		4.65	26.77		2.55	18.89		1.94	15.95
T ₆		4.85	28.32		2.89	22.58		1.85	16.74
T ₇		3.05	17.88		1.93	12.81		1.61	10.83
Treatment	Time	Soil salt content change(g·kg ^{−1})	Soil desalination rate (%)	Time	Soil salt content change (g·kg ^{−1})	Soil desalination rate (%)	Time	Soil salt content change (g·kg ^{−1})	Soil desalination rate (%)
T ₁	3 May 2020	1.69	18.30	28 June 2020	1.36	14.92			
T ₂		1.92	25.59		1.49	22.38			
T ₃		2.36	37.94		1.15	25.43			
T ₄		2.09	18.04		1.54	13.38			
T ₅		2.65	23.31		1.67	15.92			
T ₆		2.59	25.59		1.75	19.63			
T ₇		2.06	17.03		1.41	11.47			

3.3. Calibration and Verification of Model Parameters

DRAINMOD model was calibrated and verified with the predicted and field measurements. For example, the groundwater level data collected in 2019 was used for model calibration, and the model parameters were adjusted within a reasonable range to minimize the difference between the predicted and measured values. In the calibration process, lateral saturated hydraulic conductivity, hydrodynamic dispersion coefficient, maximum depth of surface water, the actual distance from the surface to impermeable layer, drainage coefficient, initial groundwater depth and *PET* correction coefficient were mainly adjusted. After that, the measured groundwater level data in 2020 were used to verify the calibrated model. The results of statistical evaluation of DRAINMOD for simulating groundwater level of 7 test plots in 2019–2020 are presented in Table 5. *MAE*, *RMSE* and *NES* were, respectively, in the range of 3.51–5.83 cm, 13.78–41.64 cm and 0.57–0.81. The simulated results of groundwater level by the 2019–2020 model were analyzed; it was found that some output items were significantly different from the measured values, and they were mainly concentrated in the time period of irrigation or rainfall. This is because the DRAINMOD model is sensitive to soil water inputs. And the model assumes that the process from leaching to production and drain into the pipes is immediate, but in practice, the process from leaching to drain took more than a few hours. In addition, the soil composition of the field was complex and presented spatial variability. The basic input data of soil profile for the model could not fully reflect the actual soil condition of the whole plot, which resulted in the failure to promptly and accurately reflect the change in the groundwater level in individual periods. However, the model performed well on the trend of the groundwater level in annual time series. In a word, the whole simulation results were overall acceptable. The water-related outputs were used to calculate the salinity of the plot profile.

Table 5. Evaluation of model simulation accuracy.

Treatment	2019			2020		
	MAE (cm)	RMSE (cm)	NSE	MAE (cm)	RMSE (cm)	NSE
T ₁	4.11	21.65	0.76	3.82	16.01	0.81
T ₂	4.37	20.35	0.71	3.51	13.78	0.70
T ₃	5.07	28.29	0.69	4.54	22.98	0.78
T ₄	4.74	24.61	0.62	3.85	16.37	0.80
T ₅	5.25	29.51	0.64	4.16	18.98	0.69
T ₆	5.83	38.32	0.57	4.77	24.97	0.75
T ₇	6.15	41.64	0.60	5.01	36.90	0.69

Note: *NSE*, Nash–Sutcliffe efficiency coefficient; *MAE*, mean absolute error; *RMSE*, root mean square error.

3.4. Soil Salts Simulation with DRAINMOD Model

The salt content of soil in the 0–100 cm layer in 2019 and 2020 was simulated and compared with the measured results (Figure 4 and Table 6). The *MAE*, *RMSE* and *NSE* of soil salt content in 2019 were 0.32–1.36 g/kg, 0.40–1.41 g/kg and 0.41–0.89, respectively. The *MAE*, *RMSE* and *NSE* of soil salt content in 2020 were 0.24–1.03 g/kg, 0.30–1.11 g/kg and 0.40–0.92, respectively. From the results of statistical evaluation, it can be seen that the model is more accurate to calculate the salt of the existing test plot, and it was feasible to use this method to simulate the change in the salt profile under different layouts of the subsurface pipe, which can be used to improve the layout of the subsurface pipe. According to the simulation, the salt accumulated during each leaching interval. Since there was no utilization of shallow groundwater, the salt increase only caused via surface evaporation. In addition, the *ET* results for each plot obtained via the model during the same period were not significantly different, so the accumulated salt values of each plot had a small difference. After two years of leaching, the soil salt content decreased significantly. The leaching effect of T₃ plot was the best with an *N* of 77.12%, while the leaching effect of T₇ plot was the worst with an *N* of 36.63%. In 2019, the desalting effect was more significant than that in 2020. After four cycles of leaching in 2019, the *N* value of each plot was 33.28–67.00% from the beginning of the experiment to the end of the year, and after three cycles of leaching from the beginning of 2020 to the end of the year, the *N* of each plot was 3.48–30.70%. With the decrease in soil salt content, the *N* of each plot was also decreasing gradually. When the soil salt content decreased to a certain extent, the leaching effect of the plots with shallow burial depth and large spacing of the subsurface pipe arrangement was no longer obvious, and the *N* of T₄ and T₇ plots in the second year was only 3.48% and 5.03%. This provides a direction for the determination of buried pipe parameters and leaching scheme.

Table 6. Evaluation of simulation accuracy of soil salt content.

Treatment	2019			2020		
	MAE (g·kg ⁻¹)	RMSE (g·kg ⁻¹)	NSE	MAE (g·kg ⁻¹)	RMSE (g·kg ⁻¹)	NSE
T ₁	0.32	0.41	0.89	1.03	1.11	0.46
T ₂	0.78	0.82	0.70	0.29	0.42	0.84
T ₃	1.36	1.41	0.49	0.85	1.03	0.40
T ₄	0.34	0.40	0.86	0.24	0.30	0.92
T ₅	0.81	0.84	0.56	0.28	0.35	0.87
T ₆	1.06	1.09	0.41	0.63	0.73	0.61
T ₇	0.70	0.84	0.47	0.51	0.59	0.66

Note: *NSE*, Nash–Sutcliffe efficiency coefficient; *MAE*, mean absolute error; *RMSE*, root mean square error.

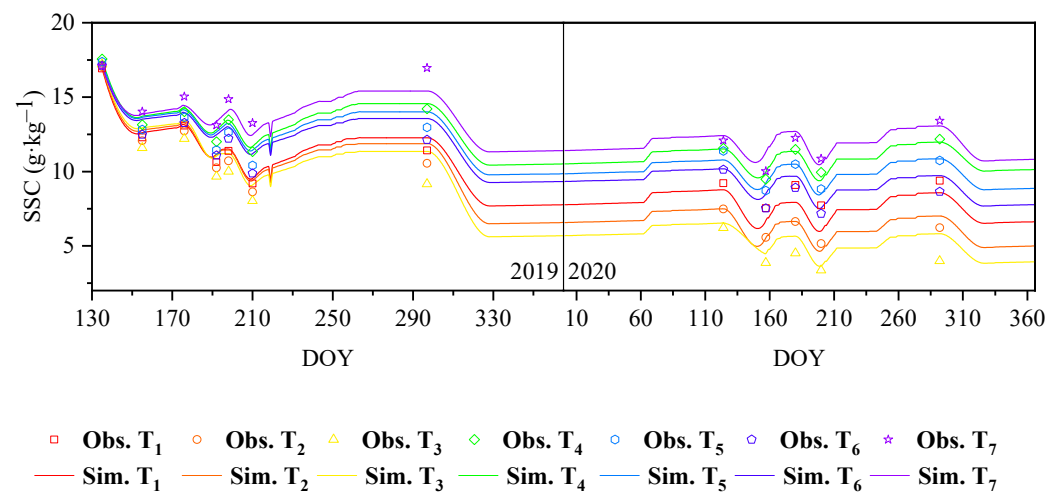


Figure 4. Simulated and measured average soil salt content (SSCs) in the 0–100 cm soil layer in each test plot in 2019 and 2020.

3.5. Soil Salt Content Simulation in Existing Plot and Predicted Plot after Sunflower Planting

The salt content changes in the 0–100 cm soil profile in the subsurface pipe control area after sunflowers planting in the existing and predicted test plots during the period 2019–2020 were simulated, respectively, and the simulation results are shown in Figure 5. The simulation showed that under the influence of shallow groundwater utilization and evapotranspiration, during the growth period of sunflowers over two years, each plot experienced a period when the soil salt content was higher than its threshold. In 2019, the days of soil salt content being higher than the threshold of salt tolerance accounted for 13.33–83.81% of the total growth period, and in 2020, the proportion was 0–93.33%. In the first year of leaching, because of the higher soil salt content, all the plots could reduce the yield of sunflower or fail to meet the growing conditions of sunflower. In the second year of leaching, the soil salt content of most plots decreased, and the time below the salt tolerance threshold of sunflowers increased. The partial test plot kept the soil salt content below the threshold of sunflower salt tolerance during the growth period, and it had no influence on the yield of sunflower. However, the phenomenon of salt accumulation in the soil in individual plots became increasingly serious, and it was difficult to meet the requirement of sunflower growth, especially in F₅ plots; the ratio of time when the salt content in the soil was above the threshold of salt tolerance to the total growth period of sunflowers increased from 83.81% to 93.33%, and sunflowers could not grow well from the seedling stage. On the one hand, these phenomena are related to the desalting capacity of each plot during leaching. On the other hand, they are related to the groundwater level caused by different layouts pipes, and the groundwater level of each plot also changed with different layouts of pipes. The deeper the subsurface pipe is, the smaller the spacing is, and the deeper the groundwater level is during the growth of sunflower. During the irrigation period, the utilization of groundwater by sunflower decreased, and the salt above the underground water entering the subsurface pipe also decreased. Therefore, the soil salt content in the experimental plot was kept below the salt tolerance threshold during the growth of sunflower. In conclusion, the normal growth conditions of sunflowers could not be satisfied after only one year of leaching. In the second year, sunflower could be successfully planted in some plots without reducing production. In the shallower and more interspaced plots, when sunflower used groundwater, the soil salt content did not decrease, and serious salt accumulation occurred. Therefore, in the improvement of the heavily saline–alkali land in Hetao Irrigation District, the layout parameters of the subsurface pipe with deeper burial depth and smaller spacing should be selected, which can not only achieve good salt leaching effect in the irrigation process, but also have a significant

inhibition effect on soil salt accumulation during the non-leaching period, so that crops can grow normally, and the yield will not be affected.

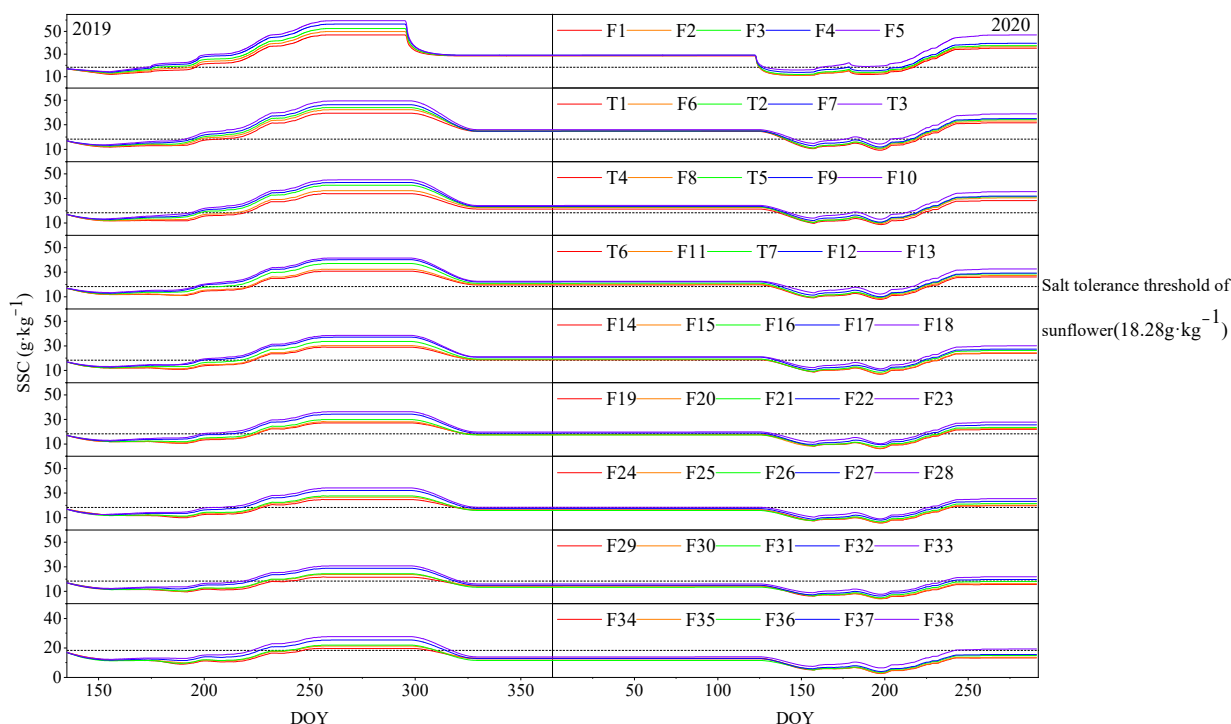


Figure 5. Simulation of average soil salt content (SSCs) in 0–100 cm soil layer after planting sunflower in existing and predicted test plots in 2019 and 2020.

3.6. Analysis of Rational Layouts of Pipes

With the data of the measured and predicted drainage and salt discharge by the subsurface pipe, N was correlated with S_o , s , d and I , SCR was correlated with s , d and annual soil desalting rate (N_i) of the subsurface pipe, and a clear quantitative relationship was established (Table 7 and Figure 6).

Table 7. Multiple linear regression model test and parameter statistics of soil desalination rate under sunflower planting conditions.

Parameter	Denormalization Coefficient	Standardization Coefficient	VIF	p	R ²	F
	B	Beta				
Constant	−61.548	-	-	0.000 **		
S_o	0.390	0.157	1.481	0.000 **	0.911	F = 678.203 p = 0.000 **
I	0.254	0.868	1.228	0.000 **		
s	−0.004	−0.121	1.041	0.000 **		
d	0.151	0.209	1.212	0.000 **		

Note: **, $p < 0.01$.

According to the above research results, the buried depth of the subsurface pipe should be as deep as possible, so the buried depth of the subsurface pipe is set as the maximum excavation depth of the machine used, namely 210 cm, which is also in the recommended critical depth range for groundwater control in arid areas [34]. In order to meet different requirements of salt drainage and salt control, the optimal buried space and desalting water volume of the pipes can be obtained using the fitting Equations (22) and (23), based on the initial salt content of this experiment (16.93 g/kg) and the buried depth of the subsurface

pipe set to 210 cm, in order to keep 100% SCR of the soil in the control area during the sunflower growth period. The aim is to remove 60%, 70%, 80%, 90% and 100% soil salt from 100 cm of soil. According to the calculation, the buried spacing of the subsurface pipe should be set as 562 cm, 902 cm, 1241 cm, 1580 cm and 1919 cm, respectively, and the corresponding optimal irrigation water volume is 33.65 cm, 38.13 cm, 42.60 cm, 47.07 cm and 51.54 cm. When the target N is 100%, the required water flow is 1.53 times of that when the target N is 60%, but the number of subsurface pipes buried is only nearly 1/3 of that when the target N is 60%. In conclusion, when soil desalting target (N) is low, less water is required for irrigation, the pipe spacing can be increased, and the number of subsurface pipes buried to meet the salt control requirements in the growth period of sunflowers can be increased. When soil desalting target (N) is high, the amount of irrigation water increases, the number of buried pipes decreases, and the buried cost of subsurface pipes in the test area decreases.

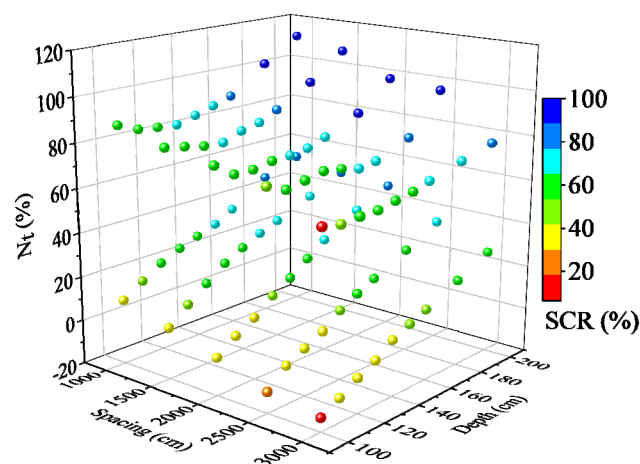


Figure 6. Relationship between salt control rate and burial depth, spacing and sum of soil desalination rate during the year.

According to the results, deep-buried subsurface pipes are beneficial to improve N . On the premise of satisfying the desalting effect, the construction cost can be reduced, and the groundwater level in the control area of pipe can be reduced. Thus, soil salinity in the root layer of the subsurface pipe control area was kept at a relatively low level, which could meet the soil conditions for crop growth. According to the initial soil salt content and construction conditions in the improved area, the optimal subsurface pipe layout parameters suitable for this area were obtained using Equations (22) and (23), Equation (23) R^2 is 0.906.

$$N = 0.390S_0 + 0.254I - 0.004s + 0.151d - 61.548 \quad (22)$$

$$SCR = 0.375d - 0.007s + 0.240N_t + 10.790 \quad (23)$$

where N is the soil desalting rate (%); S_0 is the soil salt content before leaching (g); I is the irrigation quantity (cm); s is the spacing of subsurface pipes (cm); d is the buried depth of subsurface pipes (cm); SCR is the salt control rate (%); and N_t is the total soil desalting rate in the year (%).

4. Discussion

4.1. Effects of Subsurface Pipe Drainage on Soil Moisture and Salinity

As an important drainage management measure in farmland, most studies showed that buried subsurface drainage has a great influence on the migration of soil water and salt [13,18,43]. With the increase in buried depth or the decrease in spacing, the water discharge rate of soil accelerated. Compared with the soil water content before irrigation, the soil water content after irrigation was distributed more evenly from top to bottom,

and the average soil water content decreased by $0.75 \text{ cm}^3 \text{ cm}^{-3}$ compared with that before irrigation. This is consistent with the results of Wiskow and van der Ploeg [44]. With the increase in the water displacement, the amount of salt discharged from the subsurface pipe also increases [45], and the salt concentration and N of the water discharged from the subsurface pipe are negatively correlated with the spacing, but positively correlated with the buried depth. The influence of irrigation on the 0–40 cm soil layer of different plots is greater, but the influence on the water content and salt content of the deep soil is less.

In arid and semi-arid areas where evaporation is large and groundwater level is shallow, the salt in the bottom layer will accumulate to the surface with water due to evaporation and crop transpiration after irrigation, and there is still a risk of salinization even after irrigation [46]. However, there are relatively few studies on salt accumulation in subsurface pipe test plots after irrigation. This study found that plots with good performance in irrigation can also play an effective role in inhibiting salt during non-irrigation, especially plots with the same spacing, and a large burial depth can control soil salt below the threshold of crop salt during the crop growth period. This indicates that the buried depth of the subsurface pipe has more obvious influence on the water and salt transport in soil profile than the spacing in saline–alkali soil improvement.

4.2. The Influence of Field Conditions on the Layout of Pipes

Under different soil and water environment of farmland and research objectives, the recommended layout parameters of concealed pipe will be different. When the precipitation of the study area is large and the degree of salinization is light, a shallow buried depth of the subsurface pipe is generally recommended [47,48]. In the arid and semi-arid irrigated area where this study is located, rainfall is low, and soil salinization degree is serious. In order to achieve effective salt leaching effect, it is urgent to increase the drainage and drainage amount of subsurface pipe to reduce soil salt. The results show that the buried depth of the subsurface pipe with better desalting effect in the test plot is above 1.8 m, and the soil salt content in the plot with a buried depth of 1 m increases rather than decreases during the two-year irrigation test. Therefore, based on the results of this study, it is recommended to bury the buried pipe with a depth greater than 1.8 m in saline–alkali soil improvement under current conditions. This is consistent with the findings of Qian et al., whose research showed that N is close to 0 when the buried depth of the pipe is less than 1 m [34].

Along with the increase in buried depth of subsurface pipes, it also leads to the loss of water and nutrients in soil to a certain extent, which will lead to eutrophication of drainage zone [49,50]. In order to solve this problem, on the basis of the single-layer drainage arrangement, multiple drainage methods such as double-layer drainage, controlled drainage and the combination of concealed pipe and shaft drainage were developed, which not only improved irrigation efficiency and alleviated drought stress, but also reduced nutrient loss [23,51]. However, there are few related research results of the above layout of subsurface pipe drainage, so there are certain limitations in the promotion. There are many research results on the arrangement of single-layer subsurface pipes, and the arrangement of single-layer subsurface pipe has better applicability. In this study, soil salinization can be successfully reduced, and crops can grow normally after two years of irrigation under the single-layer pipe arrangement. In order to avoid the negative effects of drought threat and nutrient loss caused by deep-buried pipes, based on the current research results, various other improvement methods can be considered, such as adding organic fertilizer and straw biochar in the field [32] or laying low permeability mulching film [52]. The improvement on the basis of not changing the layout of subsurface pipe provides a solution for the farmland that has laid subsurface pipes and encountered the above problems. The selection of the layout parameters of the subsurface pipe should be the target of the next research.

5. Conclusions

In the arid and semi-arid region of Hetao irrigation district, Inner Mongolia, the effects of subsurface pipe layout on soil salinity were studied via field experiment and numerical

simulation. The smaller the spacing and the deeper the buried pipe, the more beneficial the drainage of water and salt in soil. The influence of buried pipes on the water content and salt content of 0–40 cm surface soil is significant, and the difference of deep soil leaching in different plots is small. As the salt content of soil decreases, the more difficult it is for the salt to discharge from the soil, and the leaching effect also decreases. Based on the consideration of salt drainage and salt control, if the field conditions allow, the buried pipe should be the main buried pipe in the improvement of arid saline–alkali land. To make the results more convincing, the DRAINMOD model and drainmod equation were used to simulate the water and salt migration in soil. The results showed that *MAE*, *RMSE* and *NSE* were 0.24–1.36 g/kg, 0.30–1.41 g/kg and 0.40–0.92, respectively. The proposed method could accurately simulate the dynamic changes in soil water and salt content in the period 2019–2020. This is very beneficial to the improvement of saline–alkali land in arid and semi-arid areas. By using the calibrated model combined with the calculation of the water and salt profile, we can obtain the most suitable local concealed pipe layout parameters and the best irrigation water amount under different salt discharge and salt control objectives, which reduces the cost and greatly improves the work efficiency of the concealed pipe improvement of saline–alkali soil. The calculated pipe layout parameters can control the soil salt content below the threshold of crop salt tolerance during the crop growth period, which provides technical support for the sustainable development of farmland.

Author Contributions: F.T.: Formal analysis, Investigation, Data Curation, Formal Analysis, Visualization and Writing—Original Draft; Q.M.: Formal analysis and Investigation; H.S.: Conceptualization, Methodology, Validation, Formal analysis, Resources, Data Curation, Writing—Review and Editing, Visualization, Supervision and Project administration; R.L.: Investigation; X.D.: Investigation; J.D.: Investigation; J.L.: Writing—Review and Editing; W.F.: Writing—Review and Editing, Visualization, Supervision and funding. All authors have read and agreed to the published version of the manuscript.

Funding: The work was financially supported by the Science and Technology Major Projects of Inner Mongolia (zdx2018059), the National Natural Science Foundation of China (52269014 and 52009056), and the Research Program of Science and Technology at Universities of Inner Mongolia Autonomous Region, China (2022YFHH0044).

Data Availability Statement: The data already exist in the manuscript.

Conflicts of Interest: The authors declare that they have no known competing financial interests or personal relationships that could have appeared to influence the work reported in this paper.

References

1. Liu, Y.; Ao, C.; Zeng, W.; Kumar Srivastava, A.; Gaiser, T.; Wu, J. Simulating water and salt transport in subsurface pipe drainage systems with HYDRUS-2D. *J. Hydrol.* **2021**, *592*, 125823. [[CrossRef](#)]
2. Dregne, H.E. Land degradation in the drylands. *Arid Land Res. Manag.* **2002**, *16*, 99–132. [[CrossRef](#)]
3. Singh, A. Soil salinization and waterlogging: A threat to environment and agricultural sustainability. *Ecol. Indic.* **2015**, *57*, 128–130. [[CrossRef](#)]
4. Li, P.Y.; Wu, J.H.; Qian, H. Regulation of secondary soil salinization in semi-arid regions: A simulation research in the Nanshantaizi area along the Silk Road, northwest China. *Environ. Earth Sci.* **2016**, *75*, 698. [[CrossRef](#)]
5. Feng, W.Y.; Wang, T.K.; Zhu, Y.R.; Sun, F.H.; Giesy, J.P.; Wu, F.C. Chemical composition, sources, and ecological effect of organic phosphorus in water ecosystems: A review. *Carbon Res.* **2023**, *2*, 12. [[CrossRef](#)]
6. Asfaw, E.; Suryabhagavan, K.V.; Argaw, M. Soil salinity modeling and mapping using remote sensing and GIS: The case of Wonji sugar cane irrigation farm, Ethiopia. *J. Saudi Soc. Agric. Sci.* **2018**, *17*, 250–258. [[CrossRef](#)]
7. Li, J.; Pu, L.; Han, M.; Zhu, M.; Zhang, R.; Xiang, Y. Soil salinization research in China: Advances and prospects. *J. Geogr. Sci.* **2014**, *24*, 943–960. [[CrossRef](#)]
8. Dou, X.; Shi, H.B.; Li, R.P.; Miao, Q.F.; Tian, F.; Yu, D.D. Distribution characteristics of salinity and nutrients in salinized soil profile and estimation of salt migration. *Trans. Chin. Soc. Agric.* **2022**, *53*, 279–290+330.
9. Wang, Z. *Salt Movement Trends in Cotton Fields with Long-Term Drip Irrigation under Mulch in Typical Oasis and Irrigation Management*; China Agricultural University: Beijing, China, 2014.
10. Haj-Amor, Z.; Bourri, S. Subsurface drainage system performance, soil salinization risk, and shallow groundwater dynamic under irrigation practice in an arid land. *Arabian J. Sci. Eng.* **2019**, *44*, 467–477. [[CrossRef](#)]

11. Ritzema, H.; Chultz, B. Optimizing subsurface drainage practices in irrigated agriculture in the semi-arid and arid regions: Experience from Egypt, India AND Pakistan. *Irrig. Drain.* **2011**, *60*, 360–369. [[CrossRef](#)]
12. Sharma, D.P.; Gupta, S.K. Subsurface drainage for reversing degradation of waterlogged saline lands. *Land Degrad. Dev.* **2010**, *17*, 605–614. [[CrossRef](#)]
13. He, X.L.; Liu, H.G.; Ye, J.Y.; Yang, G.; Li, M.S.; Gong, P. Comparative investigation on soil salinity leaching under subsurface drainage and ditch drainage in Xinjiang arid region. *Int. J. Agric. Biol. Eng.* **2016**, *9*, 109–118.
14. Hornbuckle, J.W.; Christen, E.W.; Faulkner, R.D. Evaluating a multi-level subsurface drainage system for improved drainage water quality. *Agric. Water Manag.* **2007**, *89*, 208–216. [[CrossRef](#)]
15. Ceuppens, J.; Wopereis, M.; Miézan, K.M. Soil salinization processes in rice irrigation schemes in the Senegal river delta. *Soil Sci. Soc. Am. J.* **1997**, *61*, 1122–1130. [[CrossRef](#)]
16. Salo, H.; Mellin, I.; Sikkilä, M.; Nurminen, J.; Äijö, H.; Paasonen-Kivekäs, M. Performance of subsurface drainage implemented with trencher and trenchless machineries. *Agric. Water Manag.* **2019**, *213*, 957–967. [[CrossRef](#)]
17. Buckland, G.D.; Bennett, D.R.; Mikalson, D.E.; Jong, E.D.; Chang, C. Soil salinization and sodication from alternate irrigations with saline-sodic water and simulated rain. *Can. J. Soil Sci.* **2002**, *82*, 297–309. [[CrossRef](#)]
18. Skaggs, R.W.; Brevé, M.A.; Gilliam, J.W. Hydrologic and water quality impacts of agricultural drainage. *Crit. Rev. Environ. Sci. Technol.* **1994**, *24*, 1–32.
19. Nozari, H.; Azadi, S.; Zali, A. Experimental study of the temporal variation of drain water salinity at different drain depths and spacing in the presence of saline groundwater. *Sustain. Water Resour. Manag.* **2018**, *4*, 887–895.
20. Šimůnek, J.; van Genuchten, M.T.; Šejna, M. Recent developments and applications of the HYDRUS computer software packages. *Vadose Zone J.* **2016**, *15*, 25. [[CrossRef](#)]
21. Bailey, R.T.; Tavakoli-Kivi, S.; Wei, X. A salinity module for SWAT to simulate salt ion fate and transport at the watershed scale. *Hydrol. Earth Syst. Sci.* **2019**, *23*, 3155–3174. [[CrossRef](#)]
22. Skaggs, R.W.; Youssef, M.A.; Chescheir, G.M. DRAINMOD: Model use, calibration, and validation. *Trans. ASABE* **2012**, *55*, 1509–1522. [[CrossRef](#)]
23. Dou, X.; Shi, H.B.; Li, R.P.; Miao, Q.F.; Yan, J.W.; Tian, F. Simulation and evaluation of soil water and salt transport under controlled subsurface drainage using HYDRUS-2D model. *Agric. Water Manag.* **2023**, *273*, 107899. [[CrossRef](#)]
24. Addab, H.; Bailey, R.T. Simulating the effect of subsurface tile drainage on watershed salinity using SWAT. *Agric. Water Manag.* **2022**, *262*. [[CrossRef](#)]
25. Hosseini, P.; Bailey, R.T. Investigating the controlling factors on salinity in soil, groundwater, and river water in a semi-arid agricultural watershed using SWAT-Salt. *Sci. Total Environ.* **2022**, *810*, 152293.
26. Luo, W.; Skaggs, R.; Madani, A.; Cizicki, S.; Mavi, A. Predicting field hydrology in cold conditions with drainmod. *Transactions of the ASAE. Trans. ASAE Soc. Agric. Eng.* **2001**, *44*, 825–834.
27. Youssef, M.A.; Skaggs, R.W.; Chescheir, G.M.; Gilliam, J.W. The nitrogen simulation model, DRAINMOD-N II. *Trans. ASABE* **2005**, *48*, 611–626. [[CrossRef](#)]
28. Askar, M.H.; Youssef, M.A.; Chescheir, G.M.; Negm, L.M.; King, K.W.; Hesterberg, D.L. DRAINMOD Simulation of macropore flow at subsurface drained agricultural fields: Model modification and field testing. *Agric. Water Manag.* **2020**, *242*, 106401. [[CrossRef](#)]
29. Moursi, H.; Youssef, M.A.; Chescheir, G.M. Development and application of DRAINMOD model for simulating crop yield and water conservation benefits of drainage water recycling. *Agric. Water Manag.* **2022**, *266*, 107592.
30. Ren, D.; Huang, G.; Huang, Q.; Ramos, T.B.; Xu, X.; Huo, Z. Modeling and assessing the function and sustainability of natural patches in salt-affected agro-ecosystems: Application to tamarisk (*Tamarix chinensis* Lour.) in Hetao, upper Yellow River basin. *J. Hydrol.* **2017**, *552*, 490–504. [[CrossRef](#)]
31. Cao, Z.D.; Zhu, T.J.; Cai, X.M. Hydro-agro-economic optimization for irrigated farming in an arid region: The Hetao Irrigation District, Inner Mongolia. *Agric. Water Manag.* **2023**, *277*, 108095. [[CrossRef](#)]
32. Feng, W.Y.; Yang, F.; Cen, R.; Liu, J.; Qu, Z.Y.; Miao, Q.F. Effects of straw biochar application on soil temperature, available nitrogen and growth of corn. *J. Environ. Manag.* **2021**, *277*, 111331. [[CrossRef](#)]
33. Feng, Z.Z.; Miao, Q.F.; Shi, H.B.; Feng, W.Y.; Li, X.Y.; Yan, J.W. Simulation of water balance and irrigation strategy of typical sand-layered farmland in the Hetao Irrigation District, China. *Agric. Water Manag.* **2023**, *280*, 108236. [[CrossRef](#)]
34. Qian, Y.Z.; Zhu, Y.; Ye, M.; Huang, J.S.; and Wu, J.W. Experiment and numerical simulation for designing layout parameters of subsurface drainage pipes in arid agricultural areas. *Agric. Water Manag.* **2021**, *243*, 106455. [[CrossRef](#)]
35. Tong, W.; Chen, X.; Wen, X.; Chen, F.; Zhang, H.; Chu, Q. Applying a salinity response function and zoning saline land for three field crops: A case study in the Hetao Irrigation District, Inner Mongolia, China. *J. Integr. Agric.* **2015**, *14*, 178–189. [[CrossRef](#)]
36. Bouwer, H.; van Schilfgaarde, J. Simplified method of predicting fall of water table in drained land. *J. Water Resour. Prot.* **1963**, *11*, 0288–0291.
37. Kirkham, D. The Poned Water Case. In *Drainage of Agricultural Lands*; Luthin, J.N., Ed.; American Society of Agronomy: Madison, WI, USA, 1957; pp. 139–181.
38. Minhas, P.S.; Ramos, T.B.; Ben-Gal, A.; Pereira, L.S. Coping with salinity in irrigated agriculture: Crop evapotranspiration and water management issues. *Agric. Water Manag.* **2020**, *227*, 105832.

39. Liu, M.H.; Shi, H.B.; Paredes, P.; Ramos, T.B.; Dai, L.P.; Feng, Z.Z.; Pereira, L.S. Estimating and partitioning maize evapotranspiration as affected by salinity using weighing lysimeters and the SIMDualKc model. *region. Agric. Water Manag.* **2022**, *261*, 107362. [[CrossRef](#)]
40. Miao, Q.F.; Rosa, R.D.; Shi, H.B.; Paredes, P.; Zhu, L.; Dai, J.X. Modeling water use, transpiration and soil evaporation of spring wheat–maize and spring wheat–sunflower relay intercropping using the dual crop coefficient approach. *Agric. Water Manag.* **2016**, *165*, 211–229. [[CrossRef](#)]
41. Rosa, R.D.; Paredes, P.; Rodrigues, G.C.; Alves, I.; Fernando, R.M.; Pereira, L.S.; Allen, R.G. Implementing the dual crop coefficient approach in interactive software. 1. Backgr. *Comput. Strategy Agric. Water Manag.* **2012**, *103*, 8–24. [[CrossRef](#)]
42. Zhang, W.Z.; Zhang, Y.F. The specific yield and pore ratio of soils. *J. Irrig. Drain.* **1983**, *2*, 1–16.
43. Luo, W.; Sands, G.R.; Youssef, M.; Strock, J.S.; Song, I.; Canelon, D. Modeling the impact of alternative drainage practices in the northern Corn-belt with DRAINMOD-NII. *Agric. Water Manag.* **2010**, *97*, 389–398. [[CrossRef](#)]
44. Wiskow, E.; van der Ploeg, R.R. Calculation of drain spacings for optimal rainstorm flood control. *J. Hydrol.* **2003**, *272*, 163–174. [[CrossRef](#)]
45. Jafari-Talukolae, M.; Shahnazari, A.; Ahmadi, Z.M.; Darzi-Naftchali, A. Drain discharge and salt load in response to subsurface drain depth and spacing in paddy fields. *J. Irrig. Drain. Eng.* **2015**, *141*, 1–6. [[CrossRef](#)]
46. Geng, X.; Boufadel, M.C. Numerical modeling of water flow and salt transport in bare saline soil subjected to evaporation. *J. Hydrol.* **2015**, *524*, 427–438. [[CrossRef](#)]
47. Ghane, E.; Askar, M.H. Predicting the effect of drain depth on profitability and hydrology of subsurface drainage systems across the eastern USA. *Agric. Water Manag.* **2021**, *258*, 107072. [[CrossRef](#)]
48. Darzi-Naftchali, A.; Motevali, A.; Keikha, M. The life cycle assessment of subsurface drainage performance under rice-canola cropping system. *Agric. Water Manag.* **2022**, *266*, 107579. [[CrossRef](#)]
49. Sands, G.R.; Song, I.; Busman, L.M.; Hansen, B.J. The effects of subsurface drainage depth and intensity on nitrate loads in the northern cornbelt. *Trans. ASABE* **2008**, *51*, 937–946. [[CrossRef](#)]
50. Krejcová, J.; Vicentini, F.; Flynn, T.; Mudrák, O.; Frouz, J. Biodiversity loss caused by subsurface pipe drainage is difficult to restore. *Ecol. Eng.* **2021**, *170*, 106336. [[CrossRef](#)]
51. Schott, L.; Lagzdins, A.; Daigh, A.L.M.; Craft, K.; Pederson, C.; Brenneman, G. Drainage water management effects over five years on water tables, drainage, and yields in southeast Iowa. *J. Soil Water Conserv.* **2017**, *72*, 251–259. [[CrossRef](#)]
52. Zhang, J.X.; Werner, A.D.; Lu, C.H. Improving salt leaching efficiency of subsurface drainage systems using low-permeability surface mulch. *Adv. Water Resour.* **2022**, *162*, 104147. [[CrossRef](#)]

Disclaimer/Publisher’s Note: The statements, opinions and data contained in all publications are solely those of the individual author(s) and contributor(s) and not of MDPI and/or the editor(s). MDPI and/or the editor(s) disclaim responsibility for any injury to people or property resulting from any ideas, methods, instructions or products referred to in the content.